

Observation of the Decay $B^\pm \rightarrow \pi^\pm \pi^0$, Study of $B^\pm \rightarrow K^\pm \pi^0$, and Search for $B^0 \rightarrow \pi^0 \pi^0$

B. Aubert,¹ R. Barate,¹ D. Boutigny,¹ J.-M. Gaillard,¹ A. Hicheur,¹ Y. Karyotakis,¹ J. P. Lees,¹ P. Robbe,¹ V. Tisserand,¹ A. Zghiche,¹ A. Palano,² A. Pompili,² J. C. Chen,³ N. D. Qi,³ G. Rong,³ P. Wang,³ Y. S. Zhu,³ G. Eigen,⁴ I. Ofte,⁴ B. Stugu,⁴ G. S. Abrams,⁵ A. W. Borgland,⁵ A. B. Breon,⁵ D. N. Brown,⁵ J. Button-Shafer,⁵ R. N. Cahn,⁵ E. Charles,⁵ M. S. Gill,⁵ A. V. Gritsan,⁵ Y. Groysman,⁵ R. G. Jacobsen,⁵ R. W. Kadel,⁵ J. Kadyk,⁵ L. T. Kerth,⁵ Yu. G. Kolomensky,⁵ J. F. Kral,⁵ G. Kukartsev,⁵ C. LeClerc,⁵ M. E. Levi,⁵ G. Lynch,⁵ L. M. Mir,⁵ P. J. Oddone,⁵ T. J. Orimoto,⁵ M. Pripstein,⁵ N. A. Roe,⁵ A. Romosan,⁵ M. T. Ronan,⁵ V. G. Shelkov,⁵ A. V. Telnov,⁵ W. A. Wenzel,⁵ T. J. Harrison,⁶ C. M. Hawkes,⁶ D. J. Knowles,⁶ R. C. Penny,⁶ A. T. Watson,⁶ N. K. Watson,⁶ T. Deppermann,⁷ K. Goetzen,⁷ H. Koch,⁷ B. Lewandowski,⁷ M. Pelizaeus,⁷ K. Peters,⁷ H. Schmuecker,⁷ M. Steinke,⁷ N. R. Barlow,⁸ W. Bhimji,⁸ J. T. Boyd,⁸ N. Chevalier,⁸ P. J. Clark,⁸ W. N. Cottingham,⁸ C. Mackay,⁸ F. F. Wilson,⁸ C. Hearty,⁹ T. S. Mattison,⁹ J. A. McKenna,⁹ D. Thiessen,⁹ P. Kyberd,¹⁰ A. K. McKemey,¹⁰ V. E. Blinov,¹¹ A. D. Bukin,¹¹ V. B. Golubev,¹¹ V. N. Ivanchenko,¹¹ E. A. Kravchenko,¹¹ A. P. Onuchin,¹¹ S. I. Serednyakov,¹¹ Yu. I. Skovpen,¹¹ E. P. Solodov,¹¹ A. N. Yushkov,¹¹ D. Best,¹² M. Chao,¹² D. Kirkby,¹² A. J. Lankford,¹² M. Mandelkern,¹² S. McMahon,¹² R. K. Mommsen,¹² W. Roethel,¹² D. P. Stoker,¹² C. Buchanan,¹³ H. K. Hadavand,¹⁴ E. J. Hill,¹⁴ D. B. MacFarlane,¹⁴ H. P. Paar,¹⁴ Sh. Rahatlou,¹⁴ U. Schwanke,¹⁴ V. Sharma,¹⁴ J. W. Berryhill,¹⁵ C. Campagnari,¹⁵ B. Dahmes,¹⁵ N. Kuznetsova,¹⁵ S. L. Levy,¹⁵ O. Long,¹⁵ A. Lu,¹⁵ M. A. Mazur,¹⁵ J. D. Richman,¹⁵ W. Verkerke,¹⁵ J. Beringer,¹⁶ A. M. Eisner,¹⁶ C. A. Heusch,¹⁶ W. S. Lockman,¹⁶ T. Schalk,¹⁶ R. E. Schmitz,¹⁶ B. A. Schumm,¹⁶ A. Seiden,¹⁶ M. Turri,¹⁶ W. Walkowiak,¹⁶ D. C. Williams,¹⁶ M. G. Wilson,¹⁶ J. Albert,¹⁷ E. Chen,¹⁷ G. P. Dubois-Felsmann,¹⁷ A. Dvoretzki,¹⁷ D. G. Hitlin,¹⁷ I. Narsky,¹⁷ F. C. Porter,¹⁷ A. Ryd,¹⁷ A. Samuel,¹⁷ S. Yang,¹⁷ S. Jayatilleke,¹⁸ G. Mancinelli,¹⁸ B. T. Meadows,¹⁸ M. D. Sokoloff,¹⁸ T. Barillari,¹⁹ F. Blanc,¹⁹ P. Bloom,¹⁹ W. T. Ford,¹⁹ U. Nauenberg,¹⁹ A. Olivas,¹⁹ P. Rankin,¹⁹ J. Roy,¹⁹ J. G. Smith,¹⁹ W. C. van Hoek,¹⁹ L. Zhang,¹⁹ J. L. Harton,²⁰ T. Hu,²⁰ A. Soffer,²⁰ W. H. Toki,²⁰ R. J. Wilson,²⁰ J. Zhang,²⁰ D. Altenburg,²¹ T. Brandt,²¹ J. Brose,²¹ T. Colberg,²¹ M. Dickopp,²¹ R. S. Dubitzky,²¹ A. Hauke,²¹ H. M. Lacker,²¹ E. Maly,²¹ R. Müller-Pfefferkorn,²¹ R. Nogowski,²¹ S. Otto,²¹ K. R. Schubert,²¹ R. Schwierz,²¹ B. Spaan,²¹ L. Wilden,²¹ D. Bernard,²² G. R. Bonneaud,²² F. Brochard,²² J. Cohen-Tanugi,²² S. T'Jampens,²² Ch. Thiebaux,²² G. Vasileiadis,²² M. Verderi,²² R. Bernet,²³ A. Khan,²³ D. Lavin,²³ F. Muheim,²³ S. Playfer,²³ J. E. Swain,²³ J. Tinslay,²³ C. Borean,²⁴ C. Bozzi,²⁴ L. Piemontese,²⁴ A. Sarti,²⁴ E. Treadwell,²⁵ F. Anulli,²⁶ * R. Baldini-Ferrolì,²⁶ A. Calcaterra,²⁶ R. de Sangro,²⁶ D. Falciari,²⁶ G. Finocchiaro,²⁶ P. Patteri,²⁶ I. M. Peruzzi,²⁶ * M. Piccolo,²⁶ A. Zallo,²⁶ A. Buzzo,²⁷ R. Contri,²⁷ G. Crosetti,²⁷ M. Lo Vetere,²⁷ M. Macri,²⁷ M. R. Monge,²⁷ S. Passaggio,²⁷ F. C. Pastore,²⁷ C. Patrignani,²⁷ E. Robutti,²⁷ A. Santroni,²⁷ S. Tosi,²⁷ S. Bailey,²⁸ M. Morii,²⁸ G. J. Grenier,²⁹ S.-J. Lee,²⁹ U. Mallik,²⁹ J. Cochran,³⁰ H. B. Crawley,³⁰ J. Lamsa,³⁰ W. T. Meyer,³⁰ S. Prell,³⁰ E. I. Rosenberg,³⁰ J. Yi,³⁰ M. Davier,³¹ G. Grosdidier,³¹ A. Höcker,³¹ S. Laplace,³¹ F. Le Diberder,³¹ V. Lepeltier,³¹ A. M. Lutz,³¹ T. C. Petersen,³¹ S. Plaszczynski,³¹ M. H. Schune,³¹ L. Tantot,³¹ G. Wormser,³¹ R. M. Bionta,³² V. Brigljević,³² C. H. Cheng,³² D. J. Lange,³² D. M. Wright,³² A. J. Bevan,³³ J. R. Fry,³³ E. Gabathuler,³³ R. Gamet,³³ M. Kay,³³ D. J. Payne,³³ R. J. Sloane,³³ C. Touramanis,³³ M. L. Aspinwall,³⁴ D. A. Bowerman,³⁴ P. D. Dauncey,³⁴ U. Egede,³⁴ I. Eschrich,³⁴ G. W. Morton,³⁴ J. A. Nash,³⁴ P. Sanders,³⁴ G. P. Taylor,³⁴ J. J. Back,³⁵ G. Bellodi,³⁵ P. F. Harrison,³⁵ H. W. Shorthouse,³⁵ P. Strother,³⁵ P. B. Vidal,³⁵ G. Cowan,³⁶ H. U. Flaecher,³⁶ S. George,³⁶ M. G. Green,³⁶ A. Kurup,³⁶ C. E. Marker,³⁶ T. R. McMahon,³⁶ S. Ricciardi,³⁶ F. Salvatore,³⁶ G. Vaitsas,³⁶ M. A. Winter,³⁶ D. Brown,³⁷ C. L. Davis,³⁷ J. Allison,³⁸ R. J. Barlow,³⁸ A. C. Forti,³⁸ P. A. Hart,³⁸ F. Jackson,³⁸ G. D. Lafferty,³⁸ A. J. Lyon,³⁸ J. H. Weatherall,³⁸ J. C. Williams,³⁸ A. Farbin,³⁹ A. Jawahery,³⁹ D. Kovalskyi,³⁹ C. K. Lae,³⁹ V. Lillard,³⁹ D. A. Roberts,³⁹ G. Blaylock,⁴⁰ C. Dallapiccola,⁴⁰ K. T. Flood,⁴⁰ S. S. Hertzbach,⁴⁰ R. Kofler,⁴⁰ V. B. Koptchev,⁴⁰ T. B. Moore,⁴⁰ H. Staengle,⁴⁰ S. Willocq,⁴⁰ R. Cowan,⁴¹ G. Sciolla,⁴¹ F. Taylor,⁴¹ R. K. Yamamoto,⁴¹ D. J. J. Mangeol,⁴² M. Milek,⁴² P. M. Patel,⁴² F. Palombo,⁴³ J. M. Bauer,⁴⁴ L. Cremaldi,⁴⁴ V. Eschenburg,⁴⁴ R. Kroeger,⁴⁴ J. Reidy,⁴⁴ D. A. Sanders,⁴⁴ D. J. Summers,⁴⁴ H. W. Zhao,⁴⁴ C. Hast,⁴⁵ P. Taras,⁴⁵ H. Nicholson,⁴⁶ C. Cartaro,⁴⁷ N. Cavallo,⁴⁷ G. De Nardo,⁴⁷

F. Fabozzi,^{47,†} C. Gatto,⁴⁷ L. Lista,⁴⁷ P. Paolucci,⁴⁷ D. Piccolo,⁴⁷ C. Sciacca,⁴⁷ M. A. Baak,⁴⁸ G. Raven,⁴⁸ J. M. LoSecco,⁴⁹ T. A. Gabriel,⁵⁰ B. Brau,⁵¹ T. Pulliam,⁵¹ J. Brau,⁵² R. Frey,⁵² M. Iwasaki,⁵² C. T. Potter,⁵² N. B. Sinev,⁵² D. Strom,⁵² E. Torrence,⁵² F. Colecchia,⁵³ A. Dorigo,⁵³ F. Galeazzi,⁵³ M. Margoni,⁵³ M. Morandin,⁵³ M. Posocco,⁵³ M. Rotondo,⁵³ F. Simonetto,⁵³ R. Stroili,⁵³ G. Tiozzo,⁵³ C. Voci,⁵³ M. Benayoun,⁵⁴ H. Briand,⁵⁴ J. Chauveau,⁵⁴ P. David,⁵⁴ Ch. de la Vaissière,⁵⁴ L. Del Buono,⁵⁴ O. Hamon,⁵⁴ Ph. Leruste,⁵⁴ J. Ocariz,⁵⁴ M. Pivk,⁵⁴ L. Roos,⁵⁴ J. Stark,⁵⁴ P. F. Manfredi,⁵⁵ V. Re,⁵⁵ L. Gladney,⁵⁶ Q. H. Guo,⁵⁶ J. Panetta,⁵⁶ C. Angelini,⁵⁷ G. Batignani,⁵⁷ S. Bettarini,⁵⁷ M. Bondioli,⁵⁷ F. Bucci,⁵⁷ G. Calderini,⁵⁷ M. Carpinelli,⁵⁷ F. Forti,⁵⁷ M. A. Giorgi,⁵⁷ A. Lusiani,⁵⁷ G. Marchiori,⁵⁷ F. Martinez-Vidal,^{57,‡} M. Morganti,⁵⁷ N. Neri,⁵⁷ E. Paoloni,⁵⁷ M. Rama,⁵⁷ G. Rizzo,⁵⁷ F. Sandrelli,⁵⁷ G. Triggiani,⁵⁷ J. Walsh,⁵⁷ M. Haire,⁵⁸ D. Judd,⁵⁸ K. Paick,⁵⁸ D. E. Wagoner,⁵⁸ N. Danielson,⁵⁹ P. Elmer,⁵⁹ C. Lu,⁵⁹ V. Miftakov,⁵⁹ J. Olsen,⁵⁹ A. J. S. Smith,⁵⁹ E. W. Varnes,⁵⁹ F. Bellini,⁶⁰ G. Cavoto,^{59,60} D. del Re,⁶⁰ R. Faccini,^{14,60} F. Ferrarotto,⁶⁰ F. Ferroni,⁶⁰ M. Gaspero,⁶⁰ E. Leonardi,⁶⁰ M. A. Mazzoni,⁶⁰ S. Morganti,⁶⁰ M. Pierini,⁶⁰ G. Piredda,⁶⁰ F. Safai Tehrani,⁶⁰ M. Serra,⁶⁰ C. Voena,⁶⁰ S. Christ,⁶¹ G. Wagner,⁶¹ R. Waldi,⁶¹ T. Adye,⁶² N. De Groot,⁶² B. Franek,⁶² N. I. Geddes,⁶² G. P. Gopal,⁶² E. O. Olaiya,⁶² S. M. Xella,⁶² R. Aleksan,⁶³ S. Emery,⁶³ A. Gaidot,⁶³ S. F. Ganzhur,⁶³ P.-F. Giraud,⁶³ G. Hamel de Monchenault,⁶³ W. Kozanecki,⁶³ M. Langer,⁶³ G. W. London,⁶³ B. Mayer,⁶³ G. Schott,⁶³ G. Vasseur,⁶³ Ch. Yeche,⁶³ M. Zito,⁶³ M. V. Purohit,⁶⁴ A. W. Weidemann,⁶⁴ F. X. Yumiceva,⁶⁴ D. Aston,⁶⁵ R. Bartoldus,⁶⁵ N. Berger,⁶⁵ A. M. Boyarski,⁶⁵ O. L. Buchmueller,⁶⁵ M. R. Convery,⁶⁵ D. P. Coupal,⁶⁵ D. Dong,⁶⁵ J. Dorfan,⁶⁵ W. Dunwoodie,⁶⁵ R. C. Field,⁶⁵ T. Glanzman,⁶⁵ S. J. Gowdy,⁶⁵ E. Grauges-Pous,⁶⁵ T. Hadig,⁶⁵ V. Halyo,⁶⁵ T. Hryn'ova,⁶⁵ W. R. Innes,⁶⁵ C. P. Jessop,⁶⁵ M. H. Kelsey,⁶⁵ P. Kim,⁶⁵ M. L. Kocian,⁶⁵ U. Langenegger,⁶⁵ D. W. G. S. Leith,⁶⁵ S. Luitz,⁶⁵ V. Luth,⁶⁵ H. L. Lynch,⁶⁵ H. Marsiske,⁶⁵ S. Menke,⁶⁵ R. Messner,⁶⁵ D. R. Muller,⁶⁵ C. P. O'Grady,⁶⁵ V. E. Ozcan,⁶⁵ A. Perazzo,⁶⁵ M. Perl,⁶⁵ S. Petrak,⁶⁵ B. N. Ratcliff,⁶⁵ S. H. Robertson,⁶⁵ A. Roodman,⁶⁵ A. A. Salnikov,⁶⁵ T. Schietinger,⁶⁵ R. H. Schindler,⁶⁵ J. Schwiening,⁶⁵ G. Simi,⁶⁵ A. Snyder,⁶⁵ A. Soha,⁶⁵ J. Stelzer,⁶⁵ D. Su,⁶⁵ M. K. Sullivan,⁶⁵ H. A. Tanaka,⁶⁵ J. Va'vra,⁶⁵ S. R. Wagner,⁶⁵ M. Weaver,⁶⁵ A. J. R. Weinstein,⁶⁵ W. J. Wisniewski,⁶⁵ D. H. Wright,⁶⁵ C. C. Young,⁶⁵ P. R. Burchat,⁶⁶ T. I. Meyer,⁶⁶ C. Roat,⁶⁶ S. Ahmed,⁶⁷ W. Bugg,⁶⁸ M. Krishnamurthy,⁶⁸ S. M. Spanier,⁶⁸ R. Eckmann,⁶⁹ H. Kim,⁶⁹ J. L. Ritchie,⁶⁹ R. F. Schwitters,⁶⁹ J. M. Izen,⁷⁰ I. Kitayama,⁷⁰ X. C. Lou,⁷⁰ F. Bianchi,⁷¹ M. Bona,⁷¹ D. Gamba,⁷¹ L. Bosisio,⁷² G. Della Ricca,⁷² S. Dittongo,⁷² S. Grancagnolo,⁷² L. Lancieri,⁷² P. Poropat,^{72,§} L. Vitale,⁷² G. Vuagnin,⁷² R. S. Panvini,⁷³ Sw. Banerjee,⁷⁴ C. M. Brown,⁷⁴ D. Fortin,⁷⁴ P. D. Jackson,⁷⁴ R. Kowalewski,⁷⁴ J. M. Roney,⁷⁴ H. R. Band,⁷⁵ S. Dasu,⁷⁵ M. Datta,⁷⁵ A. M. Eichenbaum,⁷⁵ H. Hu,⁷⁵ J. R. Johnson,⁷⁵ R. Liu,⁷⁵ F. Di Lodovico,⁷⁵ A. K. Mohapatra,⁷⁵ Y. Pan,⁷⁵ R. Prepost,⁷⁵ S. J. Sekula,⁷⁵ J. H. von Wimmersperg-Toeller,⁷⁵ J. Wu,⁷⁵ S. L. Wu,⁷⁵ Z. Yu,⁷⁵ and H. Neal⁷⁶

(The BABAR Collaboration)

¹Laboratoire de Physique des Particules, F-74941 Annecy-le-Vieux, France

²Università di Bari, Dipartimento di Fisica and INFN, I-70126 Bari, Italy

³Institute of High Energy Physics, Beijing 100039, China

⁴University of Bergen, Inst. of Physics, N-5007 Bergen, Norway

⁵Lawrence Berkeley National Laboratory and University of California, Berkeley, CA 94720, USA

⁶University of Birmingham, Birmingham, B15 2TT, United Kingdom

⁷Ruhr Universität Bochum, Institut für Experimentalphysik 1, D-44780 Bochum, Germany

⁸University of Bristol, Bristol BS8 1TL, United Kingdom

⁹University of British Columbia, Vancouver, BC, Canada V6T 1Z1

¹⁰Brunel University, Uxbridge, Middlesex UB8 3PH, United Kingdom

¹¹Budker Institute of Nuclear Physics, Novosibirsk 630090, Russia

¹²University of California at Irvine, Irvine, CA 92697, USA

¹³University of California at Los Angeles, Los Angeles, CA 90024, USA

¹⁴University of California at San Diego, La Jolla, CA 92093, USA

¹⁵University of California at Santa Barbara, Santa Barbara, CA 93106, USA

¹⁶University of California at Santa Cruz, Institute for Particle Physics, Santa Cruz, CA 95064, USA

¹⁷California Institute of Technology, Pasadena, CA 91125, USA

¹⁸University of Cincinnati, Cincinnati, OH 45221, USA

¹⁹University of Colorado, Boulder, CO 80309, USA

²⁰Colorado State University, Fort Collins, CO 80523, USA

²¹Technische Universität Dresden, Institut für Kern- und Teilchenphysik, D-01062 Dresden, Germany

²²Ecole Polytechnique, LLR, F-91128 Palaiseau, France

²³University of Edinburgh, Edinburgh EH9 3JZ, United Kingdom

²⁴Università di Ferrara, Dipartimento di Fisica and INFN, I-44100 Ferrara, Italy

- ²⁵Florida A&M University, Tallahassee, FL 32307, USA
²⁶Laboratori Nazionali di Frascati dell'INFN, I-00044 Frascati, Italy
²⁷Università di Genova, Dipartimento di Fisica and INFN, I-16146 Genova, Italy
²⁸Harvard University, Cambridge, MA 02138, USA
²⁹University of Iowa, Iowa City, IA 52242, USA
³⁰Iowa State University, Ames, IA 50011-3160, USA
³¹Laboratoire de l'Accélérateur Linéaire, F-91898 Orsay, France
³²Lawrence Livermore National Laboratory, Livermore, CA 94550, USA
³³University of Liverpool, Liverpool L69 3BX, United Kingdom
³⁴University of London, Imperial College, London, SW7 2BW, United Kingdom
³⁵Queen Mary, University of London, E1 4NS, United Kingdom
³⁶University of London, Royal Holloway and Bedford New College, Egham, Surrey TW20 0EX, United Kingdom
³⁷University of Louisville, Louisville, KY 40292, USA
³⁸University of Manchester, Manchester M13 9PL, United Kingdom
³⁹University of Maryland, College Park, MD 20742, USA
⁴⁰University of Massachusetts, Amherst, MA 01003, USA
⁴¹Massachusetts Institute of Technology, Laboratory for Nuclear Science, Cambridge, MA 02139, USA
⁴²McGill University, Montréal, QC, Canada H3A 2T8
⁴³Università di Milano, Dipartimento di Fisica and INFN, I-20133 Milano, Italy
⁴⁴University of Mississippi, University, MS 38677, USA
⁴⁵Université de Montréal, Laboratoire René J. A. Lévesque, Montréal, QC, Canada H3C 3J7
⁴⁶Mount Holyoke College, South Hadley, MA 01075, USA
⁴⁷Università di Napoli Federico II, Dipartimento di Scienze Fisiche and INFN, I-80126, Napoli, Italy
⁴⁸NIKHEF, National Institute for Nuclear Physics and High Energy Physics, 1009 DB Amsterdam, The Netherlands
⁴⁹University of Notre Dame, Notre Dame, IN 46556, USA
⁵⁰Oak Ridge National Laboratory, Oak Ridge, TN 37831, USA
⁵¹Ohio State University, Columbus, OH 43210, USA
⁵²University of Oregon, Eugene, OR 97403, USA
⁵³Università di Padova, Dipartimento di Fisica and INFN, I-35131 Padova, Italy
⁵⁴Universités Paris VI et VII, Lab de Physique Nucléaire H. E., F-75252 Paris, France
⁵⁵Università di Pavia, Dipartimento di Elettronica and INFN, I-27100 Pavia, Italy
⁵⁶University of Pennsylvania, Philadelphia, PA 19104, USA
⁵⁷Università di Pisa, Dipartimento di fisica, Scuola Normale Superiore and INFN, I-56010 Pisa, Italy
⁵⁸Prairie View A&M University, Prairie View, TX 77446, USA
⁵⁹Princeton University, Princeton, NJ 08544, USA
⁶⁰Università di Roma La Sapienza, Dipartimento di Fisica and INFN, I-00185 Roma, Italy
⁶¹Universität Rostock, D-18051 Rostock, Germany
⁶²Rutherford Appleton Laboratory, Chilton, Didcot, Oxon, OX11 0QX, United Kingdom
⁶³DAPNIA, Commissariat à l'Energie Atomique/Saclay, F-91191 Gif-sur-Yvette, France
⁶⁴University of South Carolina, Columbia, SC 29208, USA
⁶⁵Stanford Linear Accelerator Center, Stanford, CA 94309, USA
⁶⁶Stanford University, Stanford, CA 94305-4060, USA
⁶⁷State Univ. of New York, Albany, NY 12222, USA
⁶⁸University of Tennessee, Knoxville, TN 37996, USA
⁶⁹University of Texas at Austin, Austin, TX 78712, USA
⁷⁰University of Texas at Dallas, Richardson, TX 75083, USA
⁷¹Università di Torino, Dipartimento di Fisica Sperimentale and INFN, I-10125 Torino, Italy
⁷²Università di Trieste, Dipartimento di Fisica and INFN, I-34127 Trieste, Italy
⁷³Vanderbilt University, Nashville, TN 37235, USA
⁷⁴University of Victoria, Victoria, BC, Canada V8W 3P6
⁷⁵University of Wisconsin, Madison, WI 53706, USA
⁷⁶Yale University, New Haven, CT 06511, USA

(Dated: February 7, 2008)

We present results for the branching fractions and charge asymmetries in $B^\pm \rightarrow h^\pm \pi^0$ (where $h^\pm = \pi^\pm, K^\pm$) and a search for the decay $B^0 \rightarrow \pi^0 \pi^0$ using a sample of approximately 88 million $B\bar{B}$ pairs collected by the BABAR detector at the PEP-II asymmetric-energy B Factory at SLAC. We measure $\mathcal{B}(B^\pm \rightarrow \pi^\pm \pi^0) = (5.5_{-0.9}^{+1.0} \pm 0.6) \times 10^{-6}$, where the first error is statistical and the second is systematic. The $B^\pm \rightarrow \pi^\pm \pi^0$ signal has a significance of 7.7σ including systematic uncertainties. We simultaneously measure the $K^\pm \pi^0$ branching fraction to be $\mathcal{B}(B^\pm \rightarrow K^\pm \pi^0) = (12.8_{-1.1}^{+1.2} \pm 1.0) \times 10^{-6}$. The charge asymmetries are $\mathcal{A}_{\pi^\pm \pi^0} = -0.03_{-0.17}^{+0.18} \pm 0.02$ and $\mathcal{A}_{K^\pm \pi^0} = -0.09 \pm 0.09 \pm 0.01$. We place a 90% confidence-level upper limit on the branching fraction $\mathcal{B}(B^0 \rightarrow \pi^0 \pi^0)$ of 3.6×10^{-6} .

PACS numbers: 13.25.Hw, 11.30.Er 12.15.Hh

The study of B meson decays into charmless hadronic final states plays an important role in the understanding of CP violation in the B system. In the Standard Model, CP violation arises from a single complex phase in the Cabibbo-Kobayashi-Maskawa quark-mixing matrix V_{ij} [1]. Measurements of the time-dependent CP -violating asymmetry in the $B^0 \rightarrow \pi^+\pi^-$ decay mode by the BABAR [2] and Belle [3] collaborations provide information on the angle $\alpha \equiv \arg[-V_{td}V_{tb}^*/V_{ud}V_{ub}^*]$ of the Unitarity Triangle. However, in contrast to the theoretically clean determination of the angle β in B^0 decays to charmonium final states [4, 5], the extraction of α in $B^0 \rightarrow \pi^+\pi^-$ is complicated by the interference of tree and penguin amplitudes with different weak phases. The shift between α_{eff} , from the measured $B^0 \rightarrow \pi^+\pi^-$ asymmetry, and α may be evaluated or constrained using measurements of the isospin-related decays $B^0(\bar{B}^0) \rightarrow \pi^0\pi^0$ and $B^\pm \rightarrow \pi^\pm\pi^0$ [6].

The CP -violating charge asymmetry for B^\pm modes, defined as

$$\mathcal{A}_{CP} \equiv \frac{|\bar{A}|^2 - |A|^2}{|\bar{A}|^2 + |A|^2}, \quad (1)$$

where A (\bar{A}) is the B^+ (B^-) decay amplitude, will deviate from zero if the tree and penguin amplitudes each have different weak and strong phases. In the Standard Model the decay $B^\pm \rightarrow \pi^\pm\pi^0$ has only a tree amplitude contribution, so no charge asymmetry is expected. Both the rate and asymmetry of the decay $B^\pm \rightarrow K^\pm\pi^0$ may constrain the value of the Unitarity Triangle angle γ . In particular, the ratio of $\mathcal{B}(B^\pm \rightarrow K^\pm\pi^0)$ and $\mathcal{B}(B^\pm \rightarrow K^0\pi^\pm)$ provides a lower bound for γ [7]. The decay $B^\pm \rightarrow K^\pm\pi^0$ can also exhibit a significant charge asymmetry; different models for hadronic B decays predict a range of values [8].

In this paper, we report on an observation of the decays $B^\pm \rightarrow \pi^\pm\pi^0$ and $B^\pm \rightarrow K^\pm\pi^0$, a measurement of their CP -violating charge asymmetries, and a search for the decay $B^0 \rightarrow \pi^0\pi^0$, using $(87.9 \pm 1.0) \times 10^6$ $B\bar{B}$ pairs collected with the BABAR detector.

BABAR is a solenoidal detector optimized for the asymmetric-energy beams at PEP-II and is described in detail in Ref. [9]. Charged particle (track) momenta are measured with a 5-layer double-sided silicon vertex tracker (SVT) and a 40-layer drift chamber (DCH) inside a 1.5 T superconducting solenoidal magnet. Photon (neutral cluster) positions and energies are measured with an electromagnetic calorimeter (EMC) consisting of 6580 CsI(Tl) crystals. Tracks are identified as pions or kaons by the Cherenkov angle θ_c measured with a detector of internally reflected Cherenkov light (DIRC).

High efficiency for recording $B\bar{B}$ events in which one B decays with low multiplicity is achieved with a two level trigger with complementary tracking and calorimetry-based trigger decisions. $B\bar{B}$ events are selected using track and neutral cluster content and event topology.

Candidate π^0 mesons are reconstructed as pairs of photons, spatially separated in the EMC, with an invariant mass within 3σ of the π^0 mass. The resolution sigma is approximately 8 MeV/ c^2 for high momentum π^0 . Photon candidates are required to be consistent with the expected lateral shower shape, not be matched to a track, and have a minimum energy of 30 MeV. To reduce the background from false π^0 candidates, the angle θ_γ between the photon momentum vector in the π^0 rest frame and the π^0 momentum vector in the laboratory frame is required to satisfy $|\cos\theta_\gamma| < 0.95$. The π^0 candidates are fitted kinematically with their mass constrained to the nominal π^0 mass.

Candidate tracks are required to be within the tracking fiducial volume, originate from the interaction point, consist of at least 12 DCH hits, and be associated with at least 6 Cherenkov photons in the DIRC.

B meson candidates are reconstructed by combining a π^0 with a pion or kaon (h^\pm) or by combining two π^0 mesons. Backgrounds arise from two sources: $B \rightarrow \rho\pi$ decays in which one pion is emitted nearly at rest in the B frame so that the remaining decay products are kinematically consistent with a $B^\pm \rightarrow \pi^\pm\pi^0$ or $B^0 \rightarrow \pi^0\pi^0$ decay, and $e^+e^- \rightarrow q\bar{q}$ ($q = u, d, s, c$) events where an h^\pm or π^0 from each quark randomly combine to mimic a B decay.

Both backgrounds are separated from signal using the kinematic constraints of B mesons produced at the $\Upsilon(4S)$. The first kinematic variable is the beam-energy substituted mass $m_{\text{ES}} = \sqrt{(s/2 + \mathbf{p}_i \cdot \mathbf{p}_B)^2/E_i^2 - \mathbf{p}_B^2}$, where \sqrt{s} is the total center-of-mass (CM) energy. (E_i, \mathbf{p}_i) is the four-momentum of the initial e^+e^- system and \mathbf{p}_B is the B momentum both in the laboratory frame. The second variable is $\Delta E = E_B - \sqrt{s}/2$, where E_B is the B candidate energy in the CM frame. The pion mass is assigned to all h^\pm candidates for the ΔE calculation.

The $B^\pm \rightarrow \rho^\pm\pi^0$ background to $B^0 \rightarrow \pi^0\pi^0$ is reduced by only using candidates with $|\Delta E| < 0.2$ GeV. Remaining $B^\pm \rightarrow \rho^\pm\pi^0$ background is further suppressed by removing candidates in which the additional π^\pm is identified. The track that gives a $\pi^\pm\pi^0$ invariant mass and m_{ES} of the $\pi^\pm\pi^0\pi^0$ combination most consistent with the ρ and B mass is selected. Requirements on the resulting $\pi^\pm\pi^0$ invariant mass and on the ΔE of the $\pi^\pm\pi^0\pi^0$ combination remove roughly 50% of the remaining $B^\pm \rightarrow \rho^\pm\pi^0$ background, with 93% efficiency for $B^0 \rightarrow \pi^0\pi^0$. Only $(0.40 \pm 0.04)\%$ of $B^\pm \rightarrow \rho^\pm\pi^0$ decays, and a negligible fraction of nonresonant $B^\pm \rightarrow \pi^\pm\pi^0\pi^0$ decays, remain after all cuts. For $B^\pm \rightarrow h^\pm\pi^0$ the $B \rightarrow \rho\pi$ background is suppressed by selecting candidates with $-0.11 < \Delta E < 0.15$ GeV.

The jet-like $q\bar{q}$ background is suppressed by requiring that the angle θ_s between the sphericity axes of the B candidate and of the remaining tracks and neutral clusters in the event, in the CM frame, satisfy $|\cos\theta_s| <$

TABLE I: The results for both $B^\pm \rightarrow h^\pm \pi^0$ and $B^0 \rightarrow \pi^0 \pi^0$ are summarized. The number of B candidates N , total detection efficiencies ϵ , fitted signal yields N_S , significances S , charge-averaged branching fractions \mathcal{B} , asymmetries \mathcal{A} , and 90% C.L. asymmetry limits are shown. Errors are statistical and systematic respectively, with the exception of ϵ whose error is purely systematic. The upper limit for the $B^0 \rightarrow \pi^0 \pi^0$ branching fraction corresponds to the 90% C.L., and the central value is shown in parentheses.

Mode	N	ϵ (%)	N_S	$S(\sigma)$	$\mathcal{B}(10^{-6})$	\mathcal{A}	$\mathcal{A}(90\% \text{C.L.})$
$\pi^\pm \pi^0$	21752	26.1 ± 1.7	$125_{-21}^{+23} \pm 10$	7.7	$5.5_{-0.9}^{+1.0} \pm 0.6$	$-0.03_{-0.17}^{+0.18} \pm 0.02$	$[-0.32, 0.27]$
$K^\pm \pi^0$		28.0 ± 2.0	$239_{-22}^{+21} \pm 6$	17.4	$12.8_{-1.1}^{+1.2} \pm 1.0$	$-0.09 \pm 0.09 \pm 0.01$	$[-0.24, 0.06]$
$\pi^0 \pi^0$	3020	16.5 ± 1.7	$23_{-9}^{+10} \text{ }_{-4}^{+8}$	2.5	$< 3.6 (1.6_{-0.6}^{+0.7} \text{ }_{-0.3}^{+0.6})$		

0.8 (0.7) for $B^\pm \rightarrow h^\pm \pi^0$ ($B^0 \rightarrow \pi^0 \pi^0$). Also, we require $m_{\text{ES}} > 5.2 \text{ GeV}/c^2$. The number of $B^\pm \rightarrow h^\pm \pi^0$ and $B^0 \rightarrow \pi^0 \pi^0$ candidates satisfying these requirements and the estimated efficiencies, obtained from simulated data, are shown in the first two columns of Table I. The simulation has been tuned to reproduce the observed track and π^0 efficiencies. The error in the estimated efficiency is dominated by the 5% systematic uncertainty in the single π^0 reconstruction efficiency.

The number of signal B candidates is determined in an extended unbinned maximum likelihood fit. The probability $\mathcal{P}_i(\vec{x}_j; \vec{\alpha}_i)$ for a signal or background hypothesis is the product of probability density functions (PDFs) for the variables \vec{x}_j given the set of parameters $\vec{\alpha}_i$. The likelihood function is given by a product over all N events and the M signal and background hypotheses:

$$\mathcal{L} = \exp \left(- \sum_{i=1}^M n_i \right) \prod_{j=1}^N \left[\sum_{i=1}^M N_i \mathcal{P}_i(\vec{x}_j; \vec{\alpha}_i) \right]. \quad (2)$$

For $B^\pm \rightarrow h^\pm \pi^0$ the probability coefficients are $N_i = \frac{1}{2}(1 - q_j \mathcal{A}_i) n_i$, where q_j is the charge of the track h and the fit parameters n_i and \mathcal{A}_i are the number of events and asymmetry for the four $\pi^+ \pi^0$ and $K^+ \pi^0$ signal and background components. For $B^0 \rightarrow \pi^0 \pi^0$ the coefficients are $N_i = n_i$ where the three n_i are the number of signal candidates, $B^\pm \rightarrow \rho^\pm \pi^0$ background and $q\bar{q}$ background. Monte Carlo simulations are used to verify that the likelihood fits are unbiased.

The variables \vec{x}_j used for $B^\pm \rightarrow h^\pm \pi^0$ are m_{ES} , ΔE , the Cherenkov angle θ_c of the h^\pm track, and a Fisher discriminant \mathcal{F} . The Fisher discriminant is given by an optimized linear combination of $\sum_i p_i$ and $\sum_i p_i |\cos \theta_i|^2$ where p_i is the momentum and θ_i is the angle with respect to the thrust axis of the B candidate, both in the CM frame, for all tracks and neutral clusters not used to reconstruct the B meson.

The PDFs for m_{ES} , ΔE , θ_c , and \mathcal{F} for the background are determined using data, while the PDFs for signal are found from a combination of simulated events and data. The m_{ES} distribution for background is modeled as a threshold function [10], whose shape parameter is a free parameter of the fit. The ΔE distribution for background

is modeled as a quadratic function whose parameters are determined from the m_{ES} sideband in data. The m_{ES} and ΔE distributions for signal are modeled as Gaussian distributions with a low-side power-law tail whose parameters are found with simulated events. The ΔE resolution is approximately 42 MeV based on simulated events and is confirmed by evaluating the resolution in a sample of $B^\pm \rightarrow D^0 \rho^\pm$ ($\rho^\pm \rightarrow \pi^\pm \pi^0$) events with an energetic π^0 . To allow for EMC energy scale variations, the mean of the ΔE PDF is a free parameter of the fit. To account for the use of the pion mass hypothesis, the mean of ΔE is shifted for the $K^\pm \pi^0$ PDFs. The \mathcal{F} distribution is modeled as a bifurcated Gaussian and a double Gaussian for signal and background respectively, whose parameters are determined for signal from simulation and for background from m_{ES} sidebands. The difference of the measured and expected values of θ_c for the pion or kaon hypothesis, divided by the uncertainty on θ_c , is modeled as a double Gaussian function. A control sample of kaon and pion tracks, from the decay $D^{*+} \rightarrow D^0 \pi^+$, $D^0 \rightarrow K^- \pi^+$, is used to parameterize σ_{θ_c} as a function of the track polar angle.

The variables \vec{x}_j used for $B^0 \rightarrow \pi^0 \pi^0$ are m_{ES} , ΔE , and another Fisher discriminant \mathcal{F}_T . The \mathcal{F}_T combines \mathcal{F} with information from the B tagging algorithm described in Ref. [4]. The tagging algorithm uniquely classifies events according to their lepton, kaon, and slow pion (from $D^{*+} \rightarrow D^0 \pi_{\text{slow}}^+$) content, using all tracks in the event. Nine event classes, in decreasing order of their background rejection, contain the following: a high momentum electron and a kaon, a high momentum muon and a kaon, a high momentum electron, a high momentum muon, a kaon and a slow pion, a well identified kaon, a slow pion, any kaon, or none of the above. These event classes are assigned an index, which is a new discriminating variable, and is combined with \mathcal{F} into a second Fisher discriminant \mathcal{F}_T , optimized using simulated events.

The m_{ES} distribution for $q\bar{q}$ background is parameterized by the same threshold function used in the $B^\pm \rightarrow h^\pm \pi^0$ analysis, where the shape parameter is determined from data with $|\cos \theta_s| > 0.9$. The ΔE distribution for $q\bar{q}$ background is modeled as a quadratic polynomial with parameters found from on-resonance data

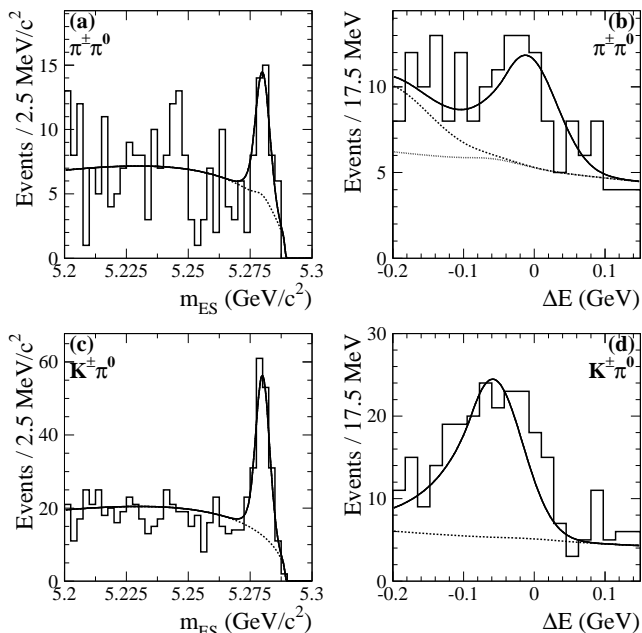


FIG. 1: The distributions of m_{ES} (left) and ΔE (right) for $B^\pm \rightarrow \pi^\pm \pi^0$ (top) and $B^\pm \rightarrow K^\pm \pi^0$ (bottom), for candidates that satisfy optimized requirements on probability ratios for signal to background based on all variables except the one being plotted. The fraction of signal events included in the plots is 24% (m_{ES}) and 35% (ΔE) for $\pi^\pm \pi^0$, and 53% (m_{ES}) and 48% (ΔE) for $K^\pm \pi^0$. Solid curves represent projections of the complete maximum likelihood fit result; dotted curves represent the background contribution. For the $B^\pm \rightarrow \pi^\pm \pi^0$ ΔE distribution, the dotted curve shows the $q\bar{q}$ background and the small $B^\pm \rightarrow K^\pm \pi^0$ cross-feed; the dashed curve includes the $B \rightarrow \rho\pi$ background as well, so is the sum of all backgrounds.

in the m_{ES} sidebands and off-resonance data. The m_{ES} and ΔE variables in both $B^0 \rightarrow \pi^0 \pi^0$ and $B^\pm \rightarrow \rho^\pm \pi^0$ are correlated, so a two dimensional PDF derived from a smoothed simulated distribution is used. The ΔE resolution is approximately 80 MeV. The \mathcal{F}_T distribution for $q\bar{q}$, $B^\pm \rightarrow \rho^\pm \pi^0$, and $B^0 \rightarrow \pi^0 \pi^0$ is modeled as the sum of three Gaussians. For $q\bar{q}$ the parameters are found using both m_{ES} sideband and off-resonance data. For $B^0 \rightarrow \pi^0 \pi^0$ and $B^\pm \rightarrow \rho^\pm \pi^0$ the parameters are found using a sample of fully reconstructed $B^0 \rightarrow D^{(*)} n \pi$ ($n = 1, 2, 3$) events.

The decay $B^\pm \rightarrow \rho^\pm \pi^0$ has not been observed; Ref. [11] set an upper limit of $\mathcal{B}(B^\pm \rightarrow \rho^\pm \pi^0) < 4.3 \times 10^{-5}$ at 90% C.L. based on a measured central value of $\mathcal{B}(B^\pm \rightarrow \rho^\pm \pi^0) = 2.4 \times 10^{-5}$. Therefore we fix the number of $B^\pm \rightarrow \rho^\pm \pi^0$ events in the fit to $n_{\rho\pi^0} = 8.4$, based on this central value, and evaluate the systematic uncertainty of allowing $n_{\rho\pi^0}$ to vary from 4.2 to 15 events.

The results of the maximum likelihood fits are summarized in Table I. Distributions of some of the variables used in the fits are shown in Figs. 1 and 2 for $B^\pm \rightarrow h^\pm \pi^0$ and $B^0 \rightarrow \pi^0 \pi^0$, respectively. The data shown are for

events that have passed a probability ratio cut optimized to enhance the signal to background fraction. The likelihood function for $B^0 \rightarrow \pi^0 \pi^0$ is shown in Fig. 2d. The statistical errors on the number of events are given by the change in signal yield n_i that corresponds to an increase in $-2 \ln \mathcal{L}$ of one unit. The systematic uncertainty in the likelihood fit is estimated by varying the PDF parameters by their statistical errors or by comparing the result with an alternate parameterization.

For $B^\pm \rightarrow \pi^\pm \pi^0$, the dominant systematic uncertainty is due to the \mathcal{F} PDF for signal (± 6.2 events) and background (± 7.6 events) PDFs, while for $B^\pm \rightarrow K^\pm \pi^0$ it is due to the m_{ES} PDF for signal (${}_{-4.6}^{+2.7}$ events). Systematic uncertainties on the CP asymmetries are evaluated from PDF parameter variations and the upper limit on intrinsic charge bias in the detector (1.0%).

For $B^0 \rightarrow \pi^0 \pi^0$, systematic uncertainties from the PDFs are due to the \mathcal{F}_T PDF for $q\bar{q}$ background (${}_{-2.4}^{+7.5}$ events), the m_{ES} PDF for $q\bar{q}$ background (${}_{-1.1}^{+1.2}$ events), and the ΔE PDF for $q\bar{q}$ background (${}_{-1.1}^{+1.0}$ events). Additional systematic uncertainties for $B^0 \rightarrow \pi^0 \pi^0$ arise from uncertainty in the EMC energy scale (${}_{-1.1}^{+0.8}$ events), the $B^\pm \rightarrow \rho^\pm \pi^0$ rejection cut (± 1.3 events), and uncertainty in the assumed $B^\pm \rightarrow \rho^\pm \pi^0$ branching fraction (${}_{-1.9}^{+1.6}$ events). The significance of the event yield, also listed in Table I, is evaluated from the square root of the change in $-2 \ln \mathcal{L}$ with the signal yield fixed to zero. The upper limit for $B^0 \rightarrow \pi^0 \pi^0$ is evaluated by finding $n_{\pi^0 \pi^0}$ where $\int_0^{n_{\pi^0 \pi^0}} \mathcal{L}(n) dn / \int_0^\infty \mathcal{L}(n) dn = 0.9$. For both significance and upper limits, systematic uncertainties are included with a worst case assumption for efficiencies and PDF variations.

We observe $\mathcal{B}(B^\pm \rightarrow \pi^\pm \pi^0) = (5.5_{-0.9}^{+1.0} \pm 0.6) \times 10^{-6}$, with a statistical significance of 7.7σ from zero. This result is consistent with several prior measurements reporting evidence for this decay [12, 13, 14]. We measure $\mathcal{B}(B^\pm \rightarrow K^\pm \pi^0) = (12.8_{-1.1}^{+1.2} \pm 1.0) \times 10^{-6}$. No evidence of direct CP violation is observed. Our limit $\mathcal{B}(B^0 \rightarrow \pi^0 \pi^0) < 3.6 \times 10^{-6}$ improves upon prior results [13, 15]. Removing correlated systematic uncertainties from luminosity and π^0 efficiency, we bound the ratio $\mathcal{B}(B^0 \rightarrow \pi^0 \pi^0) / \mathcal{B}(B^\pm \rightarrow \pi^\pm \pi^0) < 0.61$ at a 90% confidence level. Assuming isospin relations for $B \rightarrow \pi\pi$ [6], this corresponds to an upper limit of $|\alpha_{\text{eff}} - \alpha| < 51^\circ$.

We are grateful for the excellent luminosity and machine conditions provided by our PEP-II colleagues, and for the substantial dedicated effort from the computing organizations that support BABAR. The collaborating institutions wish to thank SLAC for its support and kind hospitality. This work is supported by DOE and NSF (USA), NSERC (Canada), IHEP (China), CEA and CNRS-IN2P3 (France), BMBF and DFG (Germany), INFN (Italy), FOM (The Netherlands), NFR (Norway), MIST (Russia), and PPARC (United Kingdom). Individuals have received support from the A. P. Sloan Foun-

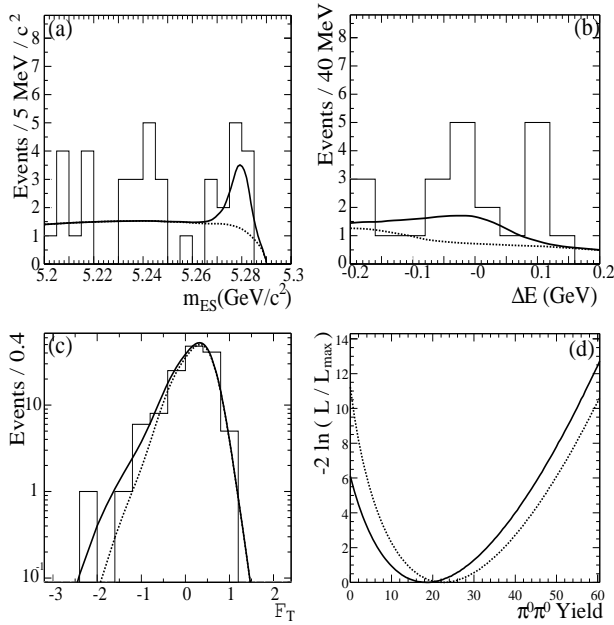


FIG. 2: The a) m_{ES} , b) ΔE , and c) \mathcal{F}_T distributions for $B^0 \rightarrow \pi^0\pi^0$ are shown, for candidates that satisfy optimized requirements on probability ratios for signal to background based on all variables except the one being plotted. The fraction of signal events included in the plots is 20%, 20% and 63% for m_{ES} , ΔE and \mathcal{F}_T , respectively. The dotted lines show the PDF projections for both $q\bar{q}$ and $B^\pm \rightarrow \rho^\pm\pi^0$ background, while the solid lines are the PDF projections for signal plus background. The ratio $-2\ln(L/L_{max})$ is shown in d) where the dashed line is for statistical errors only and the solid line is for statistical and systematic errors, as applied for the calculation of significance.

dation, Research Corporation, and Alexander von Humboldt Foundation.

* Also with Università di Perugia, Perugia, Italy

† Also with Università della Basilicata, Potenza, Italy

‡ Also with IFIC, Instituto de Física Corpuscular, CSIC-Universidad de Valencia, Valencia, Spain

§ Deceased

- [1] N. Cabibbo, Phys. Rev. Lett. **10**, 531 (1963); M. Kobayashi and T. Maskawa, Prog. Th. Phys. **49**, 652 (1973).
- [2] BABAR Collaboration, B. Aubert *et al.*, Phys. Rev. Lett. **89**, 281802 (2002).
- [3] Belle Collaboration, K. Abe *et al.*, hep-ex/0301032, submitted to Phys. Rev. D.
- [4] BABAR Collaboration, B. Aubert *et al.*, Phys. Rev. Lett. **89**, 201802 (2002).
- [5] Belle Collaboration, K. Abe *et al.*, Phys. Rev. D **66**, 071102 (2002).
- [6] M. Gronau and D. London, Phys. Rev. Lett. **65**, 3381 (1990); Y. Grossman and H.R. Quinn, Phys. Rev. D **58**, 017504 (1998); J. Charles, Phys. Rev. D **59**, 054007 (1999); M. Gronau, D. London, N. Sinha and R. Sinha, Phys. Lett. B **514**, 315 (2001).
- [7] M. Gronau and J. Rosner, Phys. Rev. D **65**, 013004 (2001).
- [8] M. Beneke, G. Buchalla, M. Neubert, and C.T. Sachrajda, Nucl. Phys. B **606**, 245 (2001); M. Ciuchini, E. Franco, G. Martinelli, M. Pierini, and L. Silvestrini, Phys. Lett. B **515**, 33 (2001); C. Isola, M. Ladsa, G. Nardulli, T.N. Pham, and P. Santorelli, Phys. Rev. D **65**, 094005 (2002); Y.Y. Keum, H.N. Li, and A.I. Sanda, Phys. Rev. D **63**, 054008 (2001).
- [9] BABAR Collaboration, B. Aubert *et al.*, Nucl. Instr. Meth. A **479**, 1 (2002).
- [10] The threshold function used for the m_{ES} PDF is $\frac{m_{ES}}{m_0} \sqrt{1 - (\frac{m_{ES}}{m_0})^2} \exp\left\{-\xi \left[1 - (\frac{m_{ES}}{m_0})^2\right]\right\}$, where m_0 is the m_{ES} endpoint, and ξ the shape parameter. See ARGUS Collaboration, H. Albrecht *et al.*, Z. Phys. C **48**, 543 (1990).
- [11] CLEO Collaboration, C.P. Jessop *et al.*, Phys. Rev. Lett. **85**, 2881 (2000).
- [12] BABAR Collaboration, B. Aubert *et al.*, Phys. Rev. Lett. **87**, 151802 (2001).
- [13] Belle Collaboration, B.C.K. Casey *et al.*, Phys. Rev. D **66**, 092002 (2002).
- [14] CLEO Collaboration, D. Cronin-Hennessy *et al.*, Phys. Rev. Lett. **85**, 515 (2000).
- [15] CLEO Collaboration, D.M. Asner *et al.*, Phys. Rev. D **65**, 031103 (2002).